JOURNAL OF CATALYSIS **100**, 45–58 (1986)

Crystallochemical Model of Active Sites on Oxide Catalysts

JACEK ZIÓŁKOWSKI

Institute of Catalysis and Surface Chemistry, Polish Academy of Sciences, 30-239 Kraków, ul. Niezapominajek, Poland

Received May 17, 1985; revised December 23, 1985

Recently the *bond strength model of active sites* (BSMAS) on oxide catalysts has been formulated (Ziółkowski, J., *J. Catal.* **81**, 311, 1983; **80**, 265, 1983; **84**, 317, 1983), based on the conviction that the pathway of catalytic reaction depends on the geometric and energetic fit between adsorbed molecule and the neighborhood of adsorption site. In terms of BSMAS structural considerations concerning various morphological planes of catalyst are found on crystallographic data and on known shapes and dimensions of molecules; bond strength is taken as a measure of binding energy. In this paper the *bond-length–bond-strength–bond-energy concept* (Ziółkowski, J., *J. Solid State Chem.* **57**, 269, 291, 1985) is used to develop BSMAS into the *crystallochemical model of active sites* (CMAS). The geometric ground of CMAS is essentially the same as that of BSMAS, while the energetic factor is expressed in the actual energy units. Applications of CMAS are illustrated by considering a number of catalytic reactions (propylene → acrolein; methanol → dimethyl ether, methylal; acetone → propylene) going on various morphological planes of MoO_3. Detailed, molecular mechanisms of these reactions are proposed as well as their energetic pathways. Assuming that the higher enthalpy of the elementary step, the higher the activation energy, the rate-determining steps are indicated. © 1986 Academic Press, Inc.

INTRODUCTION

Recently the *bond strength model of active sites* on oxide catalysts (BSMAS) has been formulated (*1–3*), inspired by Balandin's multiplet theory of heterogeneous catalysis (*4*). Concepts close to BSMAS have also been set up by Sedlaček (*5*) and Andersson (*6*). Depending on the shape and size of adsorbing molecule and the compactness of the catalyst surface there is a limited number of surface atoms with which a molecule may have a geometric contact. Some of these atoms have moreover an energetic (coordinative) undersaturation conditioning active interactions with a molecule, consisting in its adsorption and activation and in the exchange of various species between a molecule and a surface. These atoms form an active multiplet site. The identification of active multiplet sites on a catalyst surface should therefore consist in looking for a geometric and energetic correspondence between the adsorbing molecule and the neighborhood of the presumable adsorption site. As for a way of adsorption of a given molecule and its orientation with respect to the surface, available literature data can be used as discussed in (*1–3, 7*).

So far BSMAS has been developed and verified on the basis of the experimental findings involving the reactions occurring on well-defined, highly oxidized, and macroscopically flat morphological faces of catalyst grains, parallel to the respective crystallographic planes (*1–3, 7–12*). The phenomenon consisting in dependence of the mechanism of catalytic reaction on the kind of morphological plane on which the reaction occurs has been suggested to be called as *catalytic anisotropy* (*2, 3*). Therefore the model of surface of oxide catalysts has been constructed by cutting the crystal along the considered crystallographic plane in such a way as to break the weakest (i.e., the longest) bonds, to retain the configuration of atoms and bond lengths characteristic for the bulk, and to conserve the stoichiometric composition. However, taking

0021-9517/86 $3.00
Copyright © 1986 by Academic Press, Inc.
All rights of reproduction in any form reserved.

into account possible deviations from stoichiometry and the dynamics of chemisorption, some undersaturated oxygen atoms belonging to the stoichiometric surface are allowed to be absent, while some weakly bound oxygens lying over the stoichiometric surface are allowed to be present. These are conventionally called lattice and adsorbed oxygens, respectively. In other words, the positions of undersaturated oxygens are thought to be occupied statistically: the higher undersaturation, the lower population.

As for the energetic factor, *electrostatic bond strength s* (as recalled below) has been taken as a measure of binding energy and a preliminary argumentation for this assumption has been offered in (*3*). Elementary steps of catalytic reaction consisting in the exchange of oxygen or hydrogen atom between reactant and catalyst surface have been thought to proceed on the condition that

$$\Sigma s^{\text{substrate}} \lesssim \Sigma s^{\text{product}} \tag{1}$$

where sums are extended over all bonds which are formed or cut out in the considered elementary step. Inequality (1) has been tempered ($\sim$) because of simplifications involved in the model (entropy factor and surface distortions are neglected). It will be shown in this work that the energetic pathway of reaction becomes easier if some elementary steps proceed in a concerted way. Moreover, the model will be made more realistic by allowance of evidently endothermal steps, which in fact are unavoidable.

The cation–oxygen bond strength used in the above-mentioned considerations was calculated with the use of the empirical, *inverse power-type equation*

$$s = (R/R_1)^{-N} \tag{2}$$

where R is the length of a given bond and R_1 and N are the empirical constants determined for numerous cations by Brown *et al.* (*13–15*).

Recently (*16, 17*) we have proposed for the same purpose the *coulombic-type equation*[1]

$$s = \frac{dz}{R - R_0} \tag{3}$$

and we have demonstrated that so-defined bond strength is directly proportional to the bond energy E:

$$E = Js. \tag{4}$$

The symbols used in Eqs. (3) and (4) have the following meaning: z is cation valence; empirically determined d and R_0 are expressed by the formulas

$$d = 0.1350 - 0.0056z - 0.0347\,\rho_0 - 0.0050z\,\rho_0 \tag{5}$$

$$R_0 = \rho_0 + \rho_0' \tag{6}$$

ρ_0 and $\rho_0' = 0.829$ are the absolute radii of free cation and O^{2-} anion, respectively; J is equal to the standard atomization energy E_a^0 of the simple oxide M_mO_n of the considered cation forming a bond with oxygen, divided by the number m of cations in the formal molecule of this oxide and by cation valence z. All lengths and radii are expressed in Ångstroms, bond strengths in vu (valence unit), energy in kcal mol^{-1}, J in kcal mol^{-1} vu^{-1}. The values of ρ_0 are listed in (*16*) and those of J in (*17*). Combination of all these data gives

$$E = J\frac{dz}{R - R_0} = \frac{E_a^0}{m}\frac{d}{R - R_0}. \tag{7}$$

It may be useful to recall that Eqs. (3), (4), and (7) have been rationalized in terms of the *hoover model* of crystal structure. In this model, described in detail in (*16*), ions are considered to be of constant size (ρ_0, ρ_0') independently of coordination, they do not touch one another, but are maintained in space at average distances $L = R - R_0$ with electrostatic forces.

The concept outlined above makes it possible to translate BSMAS into *crystallochemical model of active sites* (CMAS) in

[1] As shown in (*16*) the numerical values of s resulting from Eqs. (2) and (3) are usually very close.

terms of which the energetic factor will be expressed in actual energy units, while the principles of geometric considerations of BSMAS remain unchanged.

BSMAS was originally formulated (in 1981) to explain the phenomenon of the *catalytic anisotropy* of the brannerite-type catalysts (solid solutions of MoO_3 in MnV_2O_6) in oxidation of propylene and *o*-xylene (*1, 3, 7, 8*). Later (*2, 3, 12*) it was extended on the catalytic transformations of propylene, methanol, ethanol, and acetone on various morphological planes of MoO_3, studied experimentally by Volta *et al.* (*9*), Tatibouët and Germain (*10, 11*) and in our laboratory (*12*). The conclusions from the BSMAS-based theoretical considerations, concerning the ascription of the reaction mechanism and products formed to the respective morphological planes remain in very good agreement with the quoted experimental findings. It was, moreover, possible to predict deoxygenation of acetone to propylene on the (100) face of molybdena (*12*). In fact, the alternative product/plane ascription in oxidation of propylene on MoO_3 (*2*) and the one-site rake reaction of *o*-xylene to C_8 products on brannerites (*7*) were also discovered after performing the theoretical considerations in terms of BSMAS. In this paper we shall not repeat the whole argumentation. As BSMAS and the newly proposed CMAS have many ideas in common, we would like to refer to paper (*3*) in which BSMAS has been described in full detail and to point out only the essential differences between these two models. As an example we intend to reconsider in terms of CMAS the mechanisms of the selected reactions developing on MoO_3. For easy comparison of various approaches the bond strength s will be calculated both with power-type and coulombic-type equations and labeled throughout this paper as s_p and s_c, respectively. The latter (s_c) will also be used to determine the *entire binding energy* of the bulk and surface atoms

$$\Sigma E = J\Sigma s_c \tag{8}$$

and the *entire undersaturation*

$$\Sigma u = \Sigma s_c^{sat} - \Sigma s_c \tag{9}$$

where Σs_c^{sat} expresses the entire strength of binding of fully saturated (bulk) atom and the sums in Eqs. (8) and (9) are extended over all existent bonds. The entire undersaturation may also be expressed in the energy units

$$\Sigma U = J\Sigma u \tag{10}$$

however, at a given Σu, ΣU may change depending on the value of J of a bond in which Σu is consumed. It seems useful to recall (*17*) that J's for Mo—O, C—O, and H—O bonds are 85.9, 96.5, and 116.0 kcal mol^{-1} vu^{-1}, respectively.

As pointed out in (*17*) Eqs. (3), (4), and (7) are also valid for oxygen-containing molecules. Therefore s_p, s_c, and E (as well as u and U if molecule is broken during the reaction) will be calculated for a number of molecules which are of interest in catalytic studies. One may believe that Eqs. (3), (4), and (7) are also valid for bonds which do not engage oxygen (C—C, C—H), however, the respective coefficients are not known at present. Fortunately average or individual bond energies of such bond can be found in the literature.

As already pointed out (*15–17*) s and E values result from the respective empirical equations and their estimated accuracy falls most frequently within 1–5%. In spite of it, all listed numerical data will be given with exaggerated accuracy to avoid an error of rounding in further calculations in which they can be used. On the other hand in considering the mechanisms of catalytic reactions the energetic data will be reasonably rounded.

All energetic considerations will be preformed as if the discussed reactions developed at normal conditions (1 atm, 298 K). At present there is no other consequent choice.

TABLE 1

Lengths[a] R, Strengths[b] s_p and s_c, and Energies[c] E of C—O, O—H, C—C, C—H, O—O, and H—H Bonds in Various Molecules

Molecule	R (Å)	s_p (vu)	s_c (vu)	E (kcal mol^{-1})
	C—O Bond			
Carbon dioxide	1.162	1.999	2.000	191.0
Carbon monoxide	1.128	2.256	2.000	256.4
Average C=O				
in aldehydes, ketones,				
esters, carboxylic acids	1.23	1.587	1.513	144.7
in conjugated systems	1.207	1.714	1.649	157.7
Average C—O				
in epoxides	1.47	0.769	0.815	77.9
in carboxylic acids	1.36	1.055	1.034	98.8
Methanol	1.427	0.868	0.889	85.0
Ethanol	1.48	0.748	0.800	76.5
Isopropanol	1.45	0.813	0.848	81.0
Formaldehyde	1.206	1.718	1.654	158.1
Acetaldehyde	1.216	1.663	1.594	152.3
Acrolein	1.21	1.696	1.630	155.9
Dimethyl ketone	1.215	1.668	1.600	152.9
Formic acid				
C=O	1.202	1.743	1.682	160.8
C—O	1.343	1.110	1.078	103.1
Ethylene oxide	1.436	0.846	0.872	83.4
Dimethyl ether	1.427	0.868	0.889	85.0
Methylal	1.42	0.885	0.902	86.2
Furan	1.362	1.048	1.029	98.3
	O—H bond			
Water	0.958	0.809	1.003	116.3
Methanol	0.956	0.813	1.019	118.2
Formic acid	0.972	0.782	0.905	105.0
	C—C bond[d]			
Average C—C				81
Average C=C				146
Average C≡C				199
	C—H bond[d]			
Average C—H				99[d]
H—CH				102
H—CH_2				110
H—CH_3				104
H—ethyl				98
H—vinyl				108
H—phenyl				110
H—allyl				89
	O—O and H—H bonds[d]			
O—O in O_2				119
H—H in H_2				104

[a] Taken form (*18, 19*).
[b] Resulting from Eqs. (2) and (3), respectively.
[c] Resulting from Eq. (7) for C—O and O—H bonds.
[d] Taken from (*20*).

RESULTS OF CALCULATIONS

1. *Molecules*

Lengths of C—O and O—H bonds in various molecules and their strengths (s_p, s_c) and energies resulting from the concepts outlined in the Introduction are listed in Table 1. Useful data for C—C, C—H, O—O, and H—H bonds, taken from the literature are also included in Table 1. Applications of these data will be discussed in one of the next paragraphs.

2. *MoO_3*

MoO_3 is orthorhombic with $a = 3.9628$, $b = 13.855$, $c = 3.6964$ Å (*21*). As shown in Fig. 1 this is a layer structure in which each layer is built up of MoO_6 octahedra at two levels, connected along c by common edges so as to form zigzag rows and along a by common corners only. In the idealized presentation (regular octahedra) each next layer bound to the former with van der Waals forces is shifted by $\frac{1}{2}(a + b)$. In fact the octahedra are markedly distorted (Fig. 1) and the deformations along a are opposite in the neighboring layers as well as within two levels belonging to the same layer. All Mo atoms are equivalent, while oxygen atoms are differentiated: O_2, O_3, and O_4 have three, two, and one Mo neighbor, respectively. Table 2 summarizes the individual lengths R, strengths (s_p, s_c), and energies E of all Mo—O bonds. Σs_p, Σs_c,

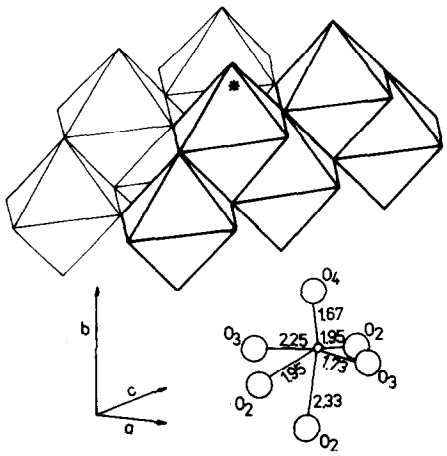

FIG. 1. Idealized presentation of a part of one layer in MoO_3 structure and the real coordination of oxygen atoms around the molybdenum atom in the octahedron marked with the asterisk.

TABLE 2

Lengths R, Strengths s_p and s_c, and Energies E of Mo—O Bonds in MoO_3

Bond	R (Å)	s_p (vu)	s_c (vu)	E (kcal mol^{-1})
Mo—O_3 (a)	1.734	1.635	1.500	128.9
Mo—O_4 (b)	1.671	2.041	2.064	177.3
Mo—O_2 (c)	2.332	0.276	0.418	35.9
Mo—$O_{3'}$ (d)	2.251	0.342	0.464	39.8
2 × Mo—$O_{2'}$ (e)	1.948	0.813	0.779	66.9

and ΣE around bulk Mo atom are 5.92 vu, 6.00 vu, and 515.7 kcal mol^{-1}, respectively. The analogous sums around O_2, O_3, and O_4 are given in Table 3.

Arrangement of atoms on various morphological faces of MoO_3 has already been discussed in (*2, 3*). These structures are shown again in Figs. 2–5 in a new presentation. The difference consists, among others, in using the absolute ρ_0 ionic radii. As they are much smaller than the previously used classical effective ionic radii (*22, 23*) the structures are more "transparent" and lower layers may be more easily visualized. Due to this fact one can easily imagine the change in the geometric and energetic situation when some of undersaturated surface atoms are absent. Geometrically and energetically nonequivalent bulk and surface oxygen atoms are distinguished

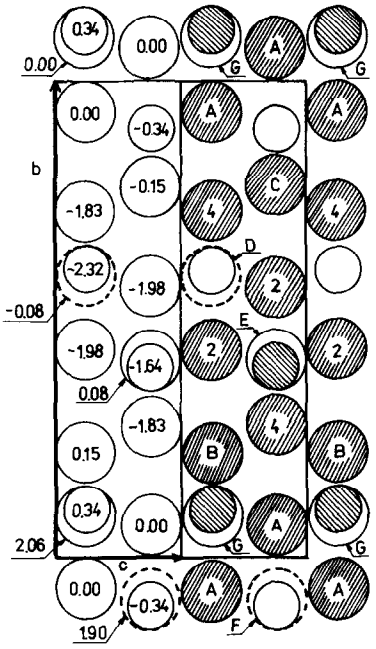

FIG. 2. Arrangement of atoms on the (100) face of MoO_3. For Figs. 2–5: Large circles, oxygen; small circles, molybdenum; proportions are based on the crystallographic data (*21*) and on the scale of the absolute ionic radii ρ_0 (*16*). In the left part of each figure the distances (in Å) of atoms from the plane are indicated. In the right part of each figure various nonequivalent bulk and surface oxygen atoms are distinguished with numbers (2, 3, 4) or letters (A, B, . . . , Z), respectively; entirely saturated atoms are dashed; "adsorbed" oxygens are drawn with dotted lines.

TABLE 3

Entire Strengths (Σs_p, Σs_c), Entire Energies (ΣE), and Undersaturation (Σu, ΣU) of All Surface and Bulk Oxygen Atoms in MoO_3

Bonds[a]	Bulk	Faces				Σs_p (vu)	Σs_c (vu)	ΣE (kcal mol^{-1})	Σu (vu)	ΣU^b (kcal mol^{-1})
		(010)	(100)	(001)	(101)					
e,e,c	O_2	O_P	O_A	—	—	1.902	1.976	169.7	—	—
a,d	O_3	O_R	—	O_K	—	1.977	1.964	168.7	—	—
b	O_4	O_S	O_B,O_C	O_L	O_Z	2.041	2.064	177.3	—	—
d	(O_3 →)[c]	—	O_D,O_F	—	—	0.342	0.464	39.8	1.500	128.9
a	(O_3 →)[c]	—	O_E,O_G	—	O_Y	1.635	1.500	128.8	0.464	39.8
c,e	(O_2 →)[c]	—	—	O_M	O_X	1.089	1.197	102.8	0.779	66.9
e	(O_2 →)[c]	—	—	O_N	—	0.813	0.779	66.9	1.197	102.8
Estim.[d]	—	—	—	—	O_W	0.276	0.418	35.9	1.582	135.9

[a] cf. Table 2.
[b] For Mo—O bonds.
[c] (O_i →) means that oxygen atoms indicated in the respective row are formed by undersaturation of the bulk O_i atom.
[d] The length of Mo—O_W bond is assumed to be the same as for the longest Mo—O_2 bond in the bulk octahedron (2.33 Å).

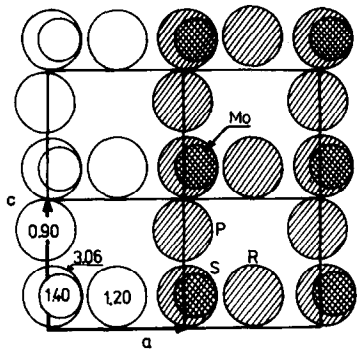

FIG. 3. Arrangement of atoms on the (010) face of MoO_3 (cf. Fig. 2).

with numbers (bulk) or letters (surface) using the same notation as in the preceeding papers. Energetic data for all surface and bulk oxygens are gathered in Table 3. Undersaturations of the surface Mo atoms are given in Table 4.

3. *Examples of Catalytic Transformations on Various Faces of MoO_3*

Figure 6 shows the assumed structure of active site on the (101) face of MoO_3 on which propylene is selectively oxidized to acrolein (*2*). Figure 7 represents the energetic changes along two possible reaction pathways. Reaction is thought to be composed of 13 elementary steps which may be grouped in stages. First (Fig. 7a) the energetic effects will be considered as if the reaction steps were independent and consecutive. Then (Fig. 7b) the most convenient energetic pathway will be searched. In searching such a pathway it will be assumed that all steps are more or less acti-

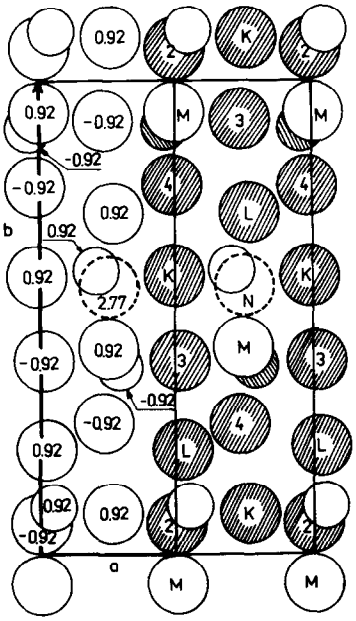

FIG. 4. Arrangement of atoms on the (001) face of MoO_3 (cf. Fig. 2).

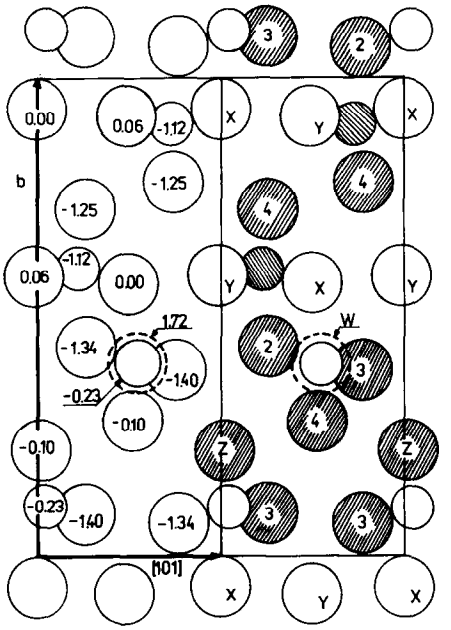

FIG. 5. Arrangement of atoms on the (101) face of MoO_3 (cf. Fig. 2).

TABLE 4

Undersaturation Σu and ΣU of Mo Atoms on Various Faces of MoO_3

Face	Molybdenum	Σu (vu)	ΣU (kcal mol^{-1})
(100)	Under vacant O_D or O_F	0.464	39.8
(100)	Under vacant O_E or O_G	1.500	128.8
(001)	Under vacant O_N	0.779	66.9
(001)	Under vacant O_M	1.197	102.8
(101)	Under vacant O_W	1.243	106.7
(010)		No undersaturated Mo	

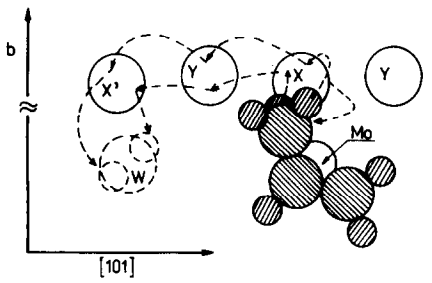

FIG. 6. Structure and performance of the active site on the (101) plane of MoO_3 converting selectively propylene to acrolein.

vated, *the higher the heat (enthalpy) of the reaction step the higher the activation energy*[2] (a negative heat of exothermal reaction is considered as a low heat). Consequently the step of the highest heat may be thought as the rate-determining step. Moreover, the energetic gains will be considered as taking place when steps are concerted. It will be also shown (Fig. 7b) that the ener-

[2] As reviewed in (*4*) large number of experimental data fulfill the formula $E_{act} = A + \gamma E$, where E is equivalent to the enthalpy of the elementary step and A and γ were found to be constant even for the reactions of various chemical nature. Although the above formula has no strict quantitative theoretical evidence it permits to assume that the higher E the higher E_{act}. This assumption should be valid at least in the case in which the steps strongly differing in E are compared.

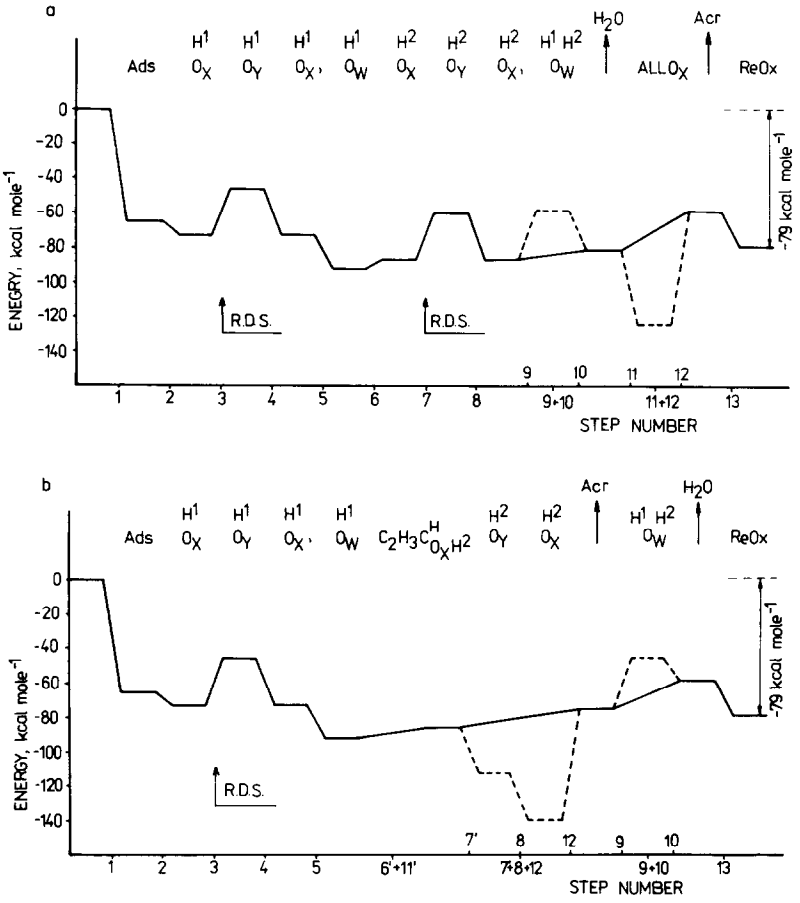

FIG. 7. Energetic pathways for oxidation of propylene to acrolein on (101) face of MoO_3 (cf. Figs. 5 and 6). Ads, adsorption; All, allyl; Acr, acrolein; ReOx, reoxidation of catalyst; ↑, desorption; two α-hydrogens are distinguished with upper indexes (H^1, H^2); surface oxygens are distinguished with lower indexes (O_X, O_Y, $O_{X'}$, O_W; cf. Fig. 6); R.D.S., rate-determining step. Dotted lines represent the steps which are thought to proceed in a concerted way.

getic effects may depend on the step sequence.

The first step (and the first stage) of oxidation of propylene consists in its adsorption in the form of π-complex over the surface undersaturated Mo atom. Undersaturation of Mo atom on the (101) face is 1.24 vu (107 kcal mol^{-1}). It is, however, hardly possible for propylene to exploit all this free binding ability of Mo atom. It seems rather that propylene can consume at most 65 kcal mol^{-1}, i.e., the difference between the energies of C=C and C—C bonds (this value is marked in Fig. 7). The second stage composed of steps 2–5 consists in the abstraction of the first α-hydrogen (H^1) and its diffusion along the row $O_XO_YO_{X'}$ to be finally localized on O_W. Step 2 requires +89 kcal mol^{-1} for abstraction of H^1, but simultaneously −97 kcal mol^{-1} are released (O_X becomes saturated, $-J_{OH} \times 1 - J_{MoO}(1.976 - 1) + 103 = -116 - 84 + 103 = -116 + 19 = -97$),[3] the result being −8 kcal mol^{-1}. In the third step O_X—H^1 is broken and O_Y—H^1 is formed ($+97 - 116 \times 1 + 129 - 85.9(1.964 - 1) = +27$, cf. footnote 3). The transfer O_Y—$H^1 \rightarrow O_{X'}$—H^1 (step 4, opposite to step 3) gives obviously −27 kcal mol^{-1} and $O_{X'}$—$H^1 \rightarrow O_W$—H^1 (step 5) gives −19 kcal mol^{-1} ($+97 - 116 = -19$). Although undersaturation of O_W is 1.582 vu it is assumed that hydrogen cannot form a bond of the strength higher than (about) 1 vu. Step 5 terminates the second stage of the reaction.

[3] It is assumed in all further calculations that: (1) if the surface oxygen atom becomes saturated its entire bond strength reaches the values of the respective bulk atom (e.g., saturated O_X behaves as O_2, $\Sigma s = 1.976$), (2) strength distribution among various bonds is so adjusted as to reach the lowest energy level (therefore in the case of saturated O_X, 1 vu is consumed by O—H bond of $J = 116$ kcal mol^{-1}, 0.976 vu is consumed by Mo—O bond of $J = 85.9$ kcal mol^{-1}, the latter bond becoming thus weaker by $103 - 85.9 \times 0.976 = 19$ kcal mol^{-1}), (3) due to the same reason ($J_{CO} = 96.5 > J_{MoO} = 85.9$) methoxyl adsorbed on the surface anion vacancy retains its strength of C—O bond of 0.889 vu and only the remaining part of Σs of oxygen may be engaged in O—Mo bond, (4) the strength of O—H bond may not be higher than 1 vu.

The third stage (Fig. 7a) involves abstraction of H^2 from allyl preformed, its movement along $O_XO_YO_{X'}O_W$ and desorption of water. It is assumed that the abstraction of the second hydrogen requires +102 kcal mol^{-1} (as for H—CH, cf. Table 1), therefore step 6 is endothermal ($+102 - 97 = +5$). Steps 7 and 8 are identical with 3 and 4, respectively. Step 9 requires +29 kcal mol^{-1} ($+97 - 0.582 \times 116 = +97 - 68 = +29$) because O_W disposes of the undersaturation of only 0.592 vu, 1 vu being already consumed[4] in step 5. Desorption of water involves the rupture of the O_W–lattice bond (+36) and formation of two O—H bonds characteristic for water (−233 diminished by the energy of the bonds already existent, i.e., $-233 + 116 + 68 = -49$; $+36 - 49 = -13$). As already pointed out in footnote 4 there is, however no necessity for water to be first formed (step 9) and only then desorbed (step 10). Therefore steps 9 and 10 are thought to proceed in a concerted way (+16), as shown in Fig. 7a with a solid line. Then we deal with the fourth stage involving the formation of acrolein (+103 for the rupture of the O_X–lattice bond and −156 due to the formation of C—O bond in acrolein; $+103 - 156 = -53$) and its desorption (+65). These two steps (11 and 12) are also considered to be concerted with the net effect of +12 kcal mol^{-1}. Finally (step 13 and fifth stage) we deal with reoxidation of the catalyst consisting in the rupture of O—O bond in O_2 (+119) and location of these two oxygens on the pair of the adjacent O_X and $O_{W'}$ vacancies (−103 and −36), where $O_{W'}$ denotes the vacancy on which propylene was originally adsorbed. As O_W has been consumed in step 10 next molecule of propylene can be adsorbed there and the reac-

[4] In this way we intend to determine mathematically the net partial energetic effect. This does not mean that O_W must form nonequivalent bonds with H^1 and H^2 (116 and 68 kcal mol^{-1}). Moreover, the requirement expressed in footnote 3 point (1) will be satisfied in the forthcoming discussion indicating that steps 9 and 10 are concerted. In reality, O_W forming two bonds with H^1 and H^2 of $s = 1$ vu has no more unexploited binding ability to be still bound to the lattice.

tion can reiterate. In this way the catalyst is brought to its initial state. The energetic result of all these steps equals −79 kcal mol^{-1} which nicely agrees with the standard enthalpy of formation of acrolein from propylene (−81 kcal mol^{-1}) thus being a good internal check of the model. As seen in Fig. 7a there are two important energetic barriers along the discussed reaction pathway joined with abstraction of H^1 and H^2.

Figure 7b shows another pathway of the same reaction which seems to be energetically more convenient. The main difference consists in the fact that steps 6′ and 11′ (highly analogous to 6 and 11) are concerted. This means that H^2-abstraction and O_X-insertion proceed simultaneously, resulting in the formation of $CH_2CHCHOH$ intermediate. We need therefore +102 and +103 kcal mol^{-1} for the rupture of C—H^2 and O_X–lattice bonds, respectively. Simultaneously −156 kcal mol^{-1} (C—O) and $-(2 - 1.63) \times 116 = -43$ kcal mol^{-1} (O—H) are released, where (2 − 1.63) is the undersaturation of oxygen in acrolein. In the next concerted step 7′ + 8 + 12 of +11 kcal mol^{-1} H^2 is transferred through O_Y to $O_{X'}$ and acrolein is desorbed. All other steps represented in Fig. 7b as well as the final heat of the reaction are the same as those in Fig. 7a. As already mentioned the reaction pathway shown in Fig. 7b is energetically more convenient and preferable as it is composed of the steps of the lower energy barriers. Abstraction of the first hydrogen (to be precise: its removal from the trap between C-O_X-O_Y) is joined with the sole high-energy barrier and brings the rate-determining step in agreement with the generally accepted ideas about the mechanism of partial oxidation of propylene. According to the scheme shown in Fig. 7b oxidation of propylene may be described as effectuated in five steps:

—adsorption of propylene;
—H^1 abstraction and its transfer to O_W;
—formation of the $C_3H_4O_XH$ intermediate and its decomposition with desorption of acrolein;
—transfer of H^2 to O_W and desorption of water;
—reoxidation of the catalyst.

It seems of interest to recall after (*2*) that the selective formation of acrolein on the (101) face of MoO_3 is mainly due to the fact that there is only one active, undersaturated oxygen in the nearest vicinity of the adsorbed propylene. As shown in(*2*) (cf. also Figs. 2 and 4) the geometrical and energetical situation on the face (001) is rather similar to that on (101) while (100) face is endowed with a high number of active oxygens around the adsorbed propylene and therefore, the formation of more oxidized products (combustion) is preferred. On the contrary, the face (010) (Fig. 3) contains only saturated Mo and O atoms and is expected to be practically inactive.

Figure 8 shows the assumed scheme of the structure and performance of the active site on the (100) face of MoO_3 (cf. Refs. (*3, 10*) and Fig. 2) on which three molecules of methanol are converted to methylal without formation of intermediary products. The respective energetic pathway is given in Fig. 9. The reaction is considered to be composed of 12 steps. The first step consists in dissociative adsorption of the first molecule of methanol with location of hydrogen on O_G and methoxyl on vacant O_F position. This requires +118 kcal mol^{-1} for the rupture of O—H bond in methanol, but simultaneously −40 and −70 kcal mol^{-1} are released due to the formation of the CH_3O_F–lattice bond ($-85.9 \times 0.464 = -40$) and O_G—H bond ($-116 + 129 - (1.964 - 1) \times 85.9 = -116 + 129 - 83 = -116 + 46 = -70$; cf. footnote 3 and the analogous bond strength redistribution in the case of the oxidation of propylene). The net effect of this step is therefore +8 kcal mol^{-1}. Step 2 consists in the nondissociative adsorption of the second methanol on the adjacent vacant O_F position in which −5 kcal mol^{-1} are released (undersaturation of oxygen in methanol). Step 3 involves the formation and desorption of water H_2O_G. For this purpose we need to break O_G–lattice bond

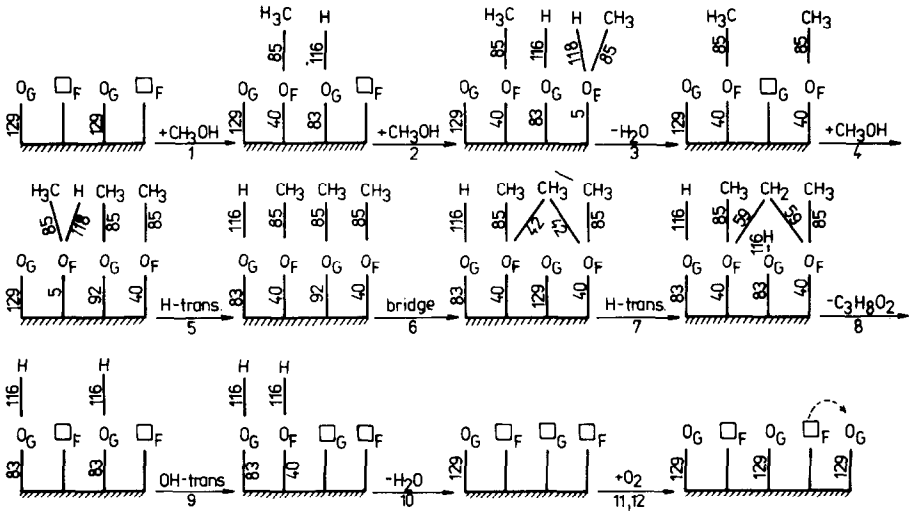

FIG. 8. Scheme of the structure and performance of the active site on the (100) face of MoO_3 on which three molecules of methanol are converted to methylal. Numbers indicate the individual bond energies in kcal mol^{-1}. Reaction is completed in twelve steps (cf. Fig. 9). Steps 11 and 12 reflect reoxidation per two molecules of methylal formed (as discussed in text); (□) vacancy.

(+83) and O_F—H bond in the second methanol (+118); at the same time two O—H bonds characteristic for water are formed (−233 diminished by already existent +116) and the energy of O_X–lattice is increased (−40 + 5 = −35), the net effect of step 3 is +49 kcal mol^{-1}. Step 4 consists in dissociative adsorption of the third methanol with location of methoxyl on the O_G vacancy and hydrogen on one of CH_3O_F methoxyls. The energetic calculations based on the same principles as explained above give −57 kcal mol^{-1} for this step (+118 − 118 − 92 + 35 = −57; strength of C—O_G bond is 0.889, energy of O_G–lattice bond is therefore diminished to −(1.964 − 0.889) × 85.9 = −92). Then we deal with the transfer of the latter mentioned hydrogen from O_F to O_G (+13). The steps 6, 7, and 8 which may be considered as consecutive or concerted (see Fig. 8) consist in formation of the O_F—CH_3—O_F bridge (−37),

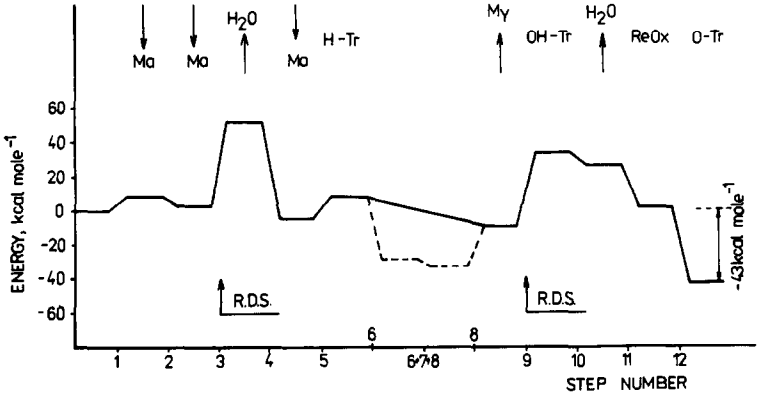

FIG. 9. Energetic pathway for conversion of three molecules of methanol to methylal (Cf. Fig. 8). Ma, methanol; My, methylal; Tr, transfer along the surface; ↓, adsorption ↑, desorption; ReOx, reoxidation of catalyst; R.D.S., rate-determining step.

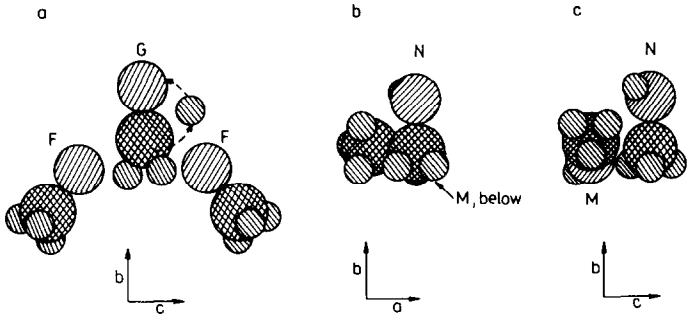

FIG. 10. Approximative conformation of the molecules of methanol (methoxyl) on the (100) face of MoO_3 (a) and on the (001) face of MoO_3 (b) and the side view of the latter (c).

H-transfer from CH_3 to O_G (−4) and desorption of methylal (+24). These apparently complicated steps are favored (3) by the particular geometry of the system shown in Fig. 10a. Namely, three methoxyls anchored on the adjacent $O_FO_GO_F$ positions have the possibility to form the angular conformation, so that carbon atom of the central one is located very close to oxygens of both side methoxyls. Step 9 (+43) involves the transfer of OH group $O_GH \rightarrow O_FH$ and step 10 (−7) consists in the formation and desorption of the second molecule of water. Finally (steps 11 and 12) we deal with reoxidation of catalyst with two oxygens (from O_2) first localized on the pair of the adjacent O_G and O_F vacancies, the latter being then transferred to the next O_G position. It should be stressed that only one oxygen is necessary for the catalyst to be brought to the initial state. Therefore steps 11 and 12 represented in Fig. 8 concern the reoxidation per two methylals formed, while twice less energetic effects marked in Fig. 9 are calculated per one $C_3H_8O_2$. They are −25 kcal mol^{-1} (step 11) and −45 kcal mol^{-1} (step 12). The final heat of the reaction is −43 kcal mol^{-1}. There are two important energy barriers along the discussed energetic pathway. The first is linked with desorption of the first molecule of water and the second with OH-transfer which may be considered as a substep of the formation and desorption of the second H_2O.

The reaction may be described briefly as composed of five stages:

—dissociative and nondissociative adsorption of two methanols and evolution of water;
—dissociative adsorption of the third methanol followed by H-transfer;
—formation and desorption of methylal;
—OH transfer and desorption of the second molecule of water;
—reoxidation of the catalyst combined with oxygen transfer.

It seems also noteworthy that on the (100) face of MoO_3, O_F and O_G oxygens or vacancies make the infinite zigzag rows along which several molecules of methanol may be adsorbed beside and along which H, O, or OH may move even at a long distance which result in conditions favorable for formation of methylal. This is no so for (001) face (Fig. 4) where the positions of undersaturated O_M and O_N (occupied or vacant) make the isolated pairs. Therefore only two molecules of methanol can be adsorbed there, dimethyl ether being the expected (*3*) and experimentally found (*10*) product.

The presumed reaction mechanism is shown in Fig. 11. It involves the consecutive (because of the geometrical reason, cf. Ref. (*3*) and Figs. 10b,c), nondissociative adsorption of two molecules of methanol on vacant O_M and O_N positions (twice −5 kcal mol^{-1}). Then in step 3 we deal with simultaneous exchange of H and CH_3 between O_N and O_M, resulting in formation of H_2O_N and $(CH_3)_2O_M$ or H_2O_M and $(CH_3)_2O_N$. This ex-

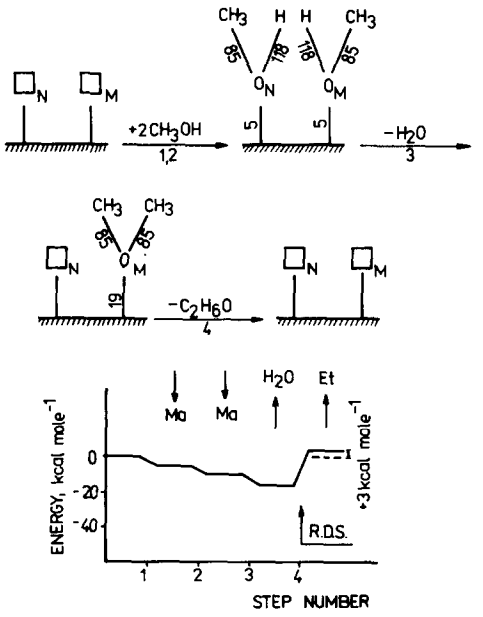

FIG. 11. Scheme of the structure and performance of the active site on the (001) face of MoO_3 converting two molecules of methanol to dimethyl ether and the energetic pathway of this reaction. Numbers indicate the individual bond energies in kcal mol^{-1}. Ma, methanol; Et, dimethyl ether; ↓, adsorption; ↑, desorption; □, vacancy; R.D.S., rate-determining step.

change is coupled with spontaneous desorption of water and gives -6 kcal mol^{-1}. Finally in step 4 dimethyl ether is desorbed which requires $+19$ kcal mol^{-1}. The last process constitutes the rate-determining step. The calculated reaction heat is $+3$ kcal mol^{-1} to be compared with the standard enthalpy equal $+1.4$ kcal mol^{-1}. Figures 10b and c show the approximate conformation of two molecules of methanol adsorbed on O_M and O_N vacancies on the (001) face of MoO_3. They are adsorbed in nearly antiparallel arrangement so that CH_3 group of one CH_3OH is located very close to the oxygen atom of the second methanol. This facilitates the transfer of CH_3 between methanols. Exchange of hydrogen may be effectuated either directly or with the intermediation of carbon.

Finally (Fig. 12) let us consider the structure and performance of the active site on the (100) face of MoO_3 on which acetone is deoxygenated to propylene(*12*). The reaction is considered to be composed of deoxygenation of acetone on O_G vacancy ($+153 - 129 = +24$) and isomerization and desorption of the intermediate formed. The latter process involves the abstraction of hydrogen from the lateral CH_3 and its transfer to the central carbon. It is assumed that this process gives -65 kcal mol^{-1} due to the formation of C=C double bond and moreover about -10 kcal mol^{-1} as hydrogen is usually more firmly bound to C= than to C—. The initial state of catalyst is reestablished by consuming O_G (which remained on the surface) in the reaction of combustion of a part of acetone which always follows its deoxygenation (*12*). Combustion is certainly composed of several steps which can not be discussed in detail at present. One can say only that the overall reaction is between

$$\tfrac{8}{8}C_3H_6O = C_3H_6 + \tfrac{3}{8}CO_2 + \tfrac{3}{8}H_2O \quad (11)$$

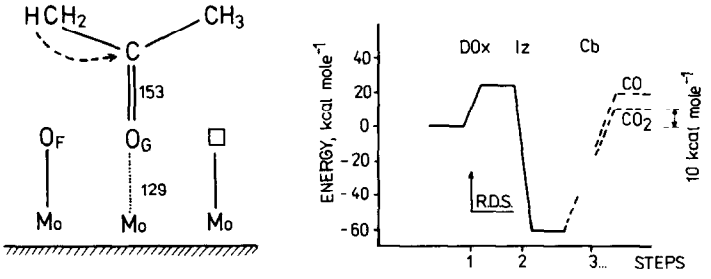

FIG. 12. Scheme of the active site on the (100) plane of MoO_3 on which acetone is deoxygenated to propylene with simultaneous combustion (as explained in the text) and energetic pathway of this reaction. DOx, deoxygenation, Iz, izomerization; Cb, combustion (being completed in a number of steps which are not considered); □, vacancy; R.D.S., rate-determining step.

and

$$\tfrac{6}{5}C_3H_6O = C_3H_6 + \tfrac{3}{5}CO + \tfrac{3}{5}H_2O \quad (12)$$

the heats being +10.7 and +19.2 kcal mol^{-1}, respectively.

CONCLUSIONS

In this paper the previously formulated (*1–3*) *bond strength model of active sites* (BSMAS) is translated and developed into the *crystallochemical model of active sites* (CMAS). In terms of CMAS the principles of geometric considerations of BSMAS based on crystallographic data remain unchanged while the energetic factor is expressed in actual energy units. For this purpose, the *bond-length–bond-strength–bond-energy concept* (*16, 17*) for cation–oxygen bonds (including C—O and O—H bonds) is utilized as well as the literature data of the bond energies of C—C, C—H, H—H, and O—O bonds in molecules. Due to this fact reaction mechanisms may be discussed in much more detail as compared to BSMAS.

The geometric factor determines the number and configuration of undersaturated surface atoms around the adsorbed molecule conditioning active interactions between them. Each catalytic reaction is thought to be composed of a number of elementary steps in which usually one bond is broken and another formed (e.g., abstraction of α-hydrogen from propylene and its binding to the surface oxygen atom). However, *some elementary steps may be concerted* which results in an energetic gain (e.g., abstraction of the second hydrogen from allyle with simultaneous insertion of oxygen resulting in formation of CH_2CH CHOH intermediate). The *algebraic sum of the energies of the broken and formed bonds gives the net energy of the (single or concerted) elementary step.* By considering a set of the consecutive steps one can construct the energetic pathway of the reaction. Each elementary step is thought to be more or less activated. Assuming that *the higher the enthalpy of the reaction step the higher its activation energy*, one can identify the most important energetic barriers along the reaction pathway and in particular the *rate-determining step.*

Certainly each reaction may be considered to be composed of steps which either differ in their chemical nature of proceed in various sequences; an example was given in the preceding paragraph (Figs. 7a,b). This results in different energetic pathways. *The most probable is that pathway along which the energy barriers are the smallest.*

In the preceding paragraph a number of reactions was discussed in terms of CMAS. Although the conclusions nicely agree with the experimental findings, CMAS may be considered as a new intellectual game on the solid chessboard, which requires further experimental verification. It seems, however, noteworthy that CMAS permits at least to formulate a very detailed working hypotheses concerning the possible reaction mechanisms.

REFERENCES

1. Ziółkowski, J., *J. Catal.* **81,** 311 (1983).
2. Ziółkowski, J., *J. Catal.* **80,** 265 (1983).
3. Ziółkowski, J., *J. Catal.* **84,** 317 (1983).
4. Balandin, A. A., "Advances in Catalysis," Vol. 19, p. 1. Academic Press, New York, 1969.
5. Sedlaček, J., *J. Catal.* **57,** 208 (1979).
6. Andersson A., *J. Solid State Chem.* **42,** 263 (1982).
7. Ziółkowski, J., and Gąsior, M., *J. Catal.* **84,** 74 (1983).
8. Ziółkowski, J., and Janas, J., *J. Catal.* **81,** 289 (1983).
9. Volta, J. C., Forissier, M., Theobald, F., and Pham, T. P., *Faraday Discuss.* 72/13. Selectivity in Heterogenous Catalysis, Nottingham, 1981.
10. Tatibouët, J. M., and Germain, J. E., *J. Catal.* **72,** 385 (1981).
11. Tatibouët, J. M., and Germain, J. E., *J. Chem. Res. Synop.*, 286 (1981); *J. Chem. Res. Miniprint*, 3070 (1981).
12. Ziółkowski, J., and Wiltowski, T., *J. Catal.* **90,** 329 (1984).
13. Brown, I. D., and Shannon, R. D., *Acta Crystallogr. Sect. A* **29,** 266 (1973).
14. Brown, I. D., and Wu, K. K., *Acta Crystallogr. Sect. B* **32,** 1957 (1976).
15. Brown, I. D., *in* "Structure and Bonding in Crys-

tals" (M. O'Keeffe and A. Navrotsky, Eds.), Vol. 2. Academic Press, New York, 1981.

16. Ziółkowski, J., *J. Solid State Chem.* **57,** 269 (1985).
17. Ziółkowski, J., and Dziembaj, L., *J. Solid State Chem.* **57,** 291 (1985).
18. CRC Handbook of Chemistry and Physics, 59th ed. 1978/79. CRC Press, West Palm Beach, Florida.
19. Sverdlov, L. M., Kovner, M. A., and Krainov, E. P., "Vibration Spectra of Complex Molecules." Nauka, Moscow, 1970.
20. Pitzer, K. P., *J. Amer. Chem. Soc.* **70,** 2140 (1948).
21. Kihlborg, L., *Ark. Kemi* **21,** 357 (1963).
22. Shannon, R. D., and Prewitt, C. T., *Acta Crystallogr. Sect. B* **25,** 925 (1969).
23. Shannon, R. D., *Acta Crystallogr. Sect. A* **32,** 751 (1976).